



**HAL**  
open science

# Deep learning approach for designing acoustic absorbing metasurfaces with high degrees of freedom

Krupali Donda, Yifan Zhu, Aurélien Merkel, Sheng Wan, Badreddine Assouar

## ► To cite this version:

Krupali Donda, Yifan Zhu, Aurélien Merkel, Sheng Wan, Badreddine Assouar. Deep learning approach for designing acoustic absorbing metasurfaces with high degrees of freedom. *Extreme Mechanics Letters*, 2022, 56, pp.101879. 10.1016/j.eml.2022.101879 . hal-03843366

**HAL Id: hal-03843366**

**<https://hal.science/hal-03843366>**

Submitted on 8 Nov 2022

**HAL** is a multi-disciplinary open access archive for the deposit and dissemination of scientific research documents, whether they are published or not. The documents may come from teaching and research institutions in France or abroad, or from public or private research centers.

L'archive ouverte pluridisciplinaire **HAL**, est destinée au dépôt et à la diffusion de documents scientifiques de niveau recherche, publiés ou non, émanant des établissements d'enseignement et de recherche français ou étrangers, des laboratoires publics ou privés.



Distributed under a Creative Commons Attribution - NonCommercial - NoDerivatives 4.0 International License

# Deep Learning Approach for Designing Acoustic Absorbing Metasurfaces with High Degrees of Freedom

Krupali Donda, Yifan Zhu, Aurélien Merkel, Sheng Wan and Badreddine Assouar\*

*Université de Lorraine, CNRS, Institut Jean Lamour, Nancy, France*

## Abstract:

The advent of the acoustic metasurfaces offered an unprecedented expansion of our ability to manipulate and structure sound waves for many exotic functionalities. However, the metasurface designs require deep expertise in acoustics and highly intensive iterative computations using Finite Element Method. In this work, we use a two-dimensional convolutional neural network to model complex metasurface absorber structures under oblique wave incidences. The proposed network architecture is capable of computing the absorption spectra with a large number of design degrees of freedom. Further, we implement a conditional generative adversarial network to solve the inverse design problem. When fed with an input set of predefined absorption spectra, the constructed generative network produces candidate designs of metasurface absorbers that match on-demand the spectra with high fidelity. We demonstrate the capability of the implemented network architecture by designing a metasurface absorber operating at 82Hz for oblique wave incidences with a thickness of  $\lambda/64$ . To implement the deep learning methods for acoustic designs, the main challenge is to generate large and high-quality training data set using numerical simulations. To mitigate this issue, we implement data augmentation. The presented approaches open new avenues to automate the design process of metasurfaces and enable a much more generalized and broader scope of optimal designs that go beyond acoustics applications.

**Keywords:** Acoustic metasurfaces, Sound absorption, Low frequency regime, Deep learning, Convolutional neural network, Conditional generative adversarial network, Inverse design.

\*Corresponding author: [badreddine.assouar@univ-lorraine.fr](mailto:badreddine.assouar@univ-lorraine.fr)

## 1. Introduction

Acoustic metasurfaces have enabled precise acoustic wave manipulation with strong potential that provides a new route to obtain unprecedented functionalities with compact geometric structure [1-4]. Such advantages in precision and functionalities come at the cost of tremendous difficulty in finding individual metasurface structures based on specific criteria, which makes design and optimization of metasurface a key challenge in the acoustic field. Current design strategies include theoretical methods [5-9], numerical simulations [8-13], optimization algorithms for the inverse designs [14-20], and deep neural networks [21-38]. Exploring designs beyond the ones that can be theoretically modeled without difficulties requires a cumbersome empirical trial and error method using simulation algorithms, usually based on the Finite Element Method (FEM). Starting from certain initial and boundary conditions, and by discretizing linearized Navier-Stokes equations, such acoustic simulations solve the design problem. The accurate acoustic response can be calculated by setting up sufficient meshes and iterations. It is frequently needed to fine-tune the structure and perform simulations iteratively to gradually approach the desired responses. This process depends on the experience of the design models and it also takes a long time, especially for low-frequency three-dimensional (3D) calculations. This is due to the narrow bandwidth at low frequencies, which necessitates a high enough resolution to sweep the frequencies for accurate calculations. In addition, large computational times arise in thermoviscous acoustics due to the necessity to fine mesh the boundary layers where momentum and heat transfers occur. With the long simulation time and thus limited exploration of the design space, the optimal solution is often overlooked.

Inverse design problems are even more difficult because they require direct retrieval of the proper structure for the desired acoustic performance, which necessitates a much larger number of Degrees Of Freedom (DOFs) in the design space. Such designs are usually based on optimization methods, most commonly either gradient-based or evolutionary-based [14-20]. These approaches enable researchers to discover non-intuitive and freeform acoustic structures which outperform empirically designed structures. These algorithms, on the other hand, are driven by rules that have iterative searching steps in a case-by-case manner and frequently rely on numerical simulations to generate intermediate results that aid in the modification of the searching strategy. The converging speed using such an approach depends on the solver which is connected to the optimizer. As a result, modeling and characterization tools play an important role in all current design processes. In this context, precise and time-efficient design methods

must be thoroughly investigated to design of next-generation acoustic metasurface devices, which are frequently characterized by large numbers of design DOFs and multifunctionalities.

Very recently, deep neural networks (DNNs) have been adopted as a radically new design tool to address forward and inverse acoustic problems. The great advantage of such learning-based models lies in their ability to model physical systems that fall outside of the training dataset. Due to such generalization capability, DNN can be used as a forward design optimization engine. In the field of acoustics, the DNNs have been implemented using fully connected layers (FCLs) and convolution layers [21-29]. Once properly trained with adequate data such deep learning models are very accurate and capable of generating desired acoustic responses on the millisecond timescale. In addition, various deep learning-based models are proposed to solve inverse acoustic problems [30-40]. Despite such development in this field, there are still challenges with the existing networks specially built using FCLs. Such kind of networks primarily deal with simple acoustic structures with a limited number of parameters, severely limiting the accessible acoustic design DOFs and because of this, current deep learning models are insufficient as a general design scheme. Also, deep learning approaches require a large amount of training data to understand the latent patterns. For designing the complex acoustics devices, the generation of the training dataset is usually dependent on the numerical simulations which leads to a substantial computational burden. It is extremely challenging to generate high-quality annotated data on a large scale using numerical simulations. The tradeoff between the size of the training dataset and the model accuracy is a critical factor to be considered. To solve this issue, we have implemented a data augmentation technique that not only increases the training dataset size but, also increases the diversity in the dataset which makes the network more robust [41,42]. Furthermore, we have implemented the dimensionality reduction technique principal component analysis (PCA). It is a statistical method that allows to significantly lower the dimensionality of data without a significant loss of information in the process which helps to accelerate the learning process [43].

The ultrathin design of acoustic metasurface absorbers for very low frequency remains a major topic in research. The prototypical designs are mostly based on educable guesses which may not always be sufficient to achieve full absorption at extremely low frequency [44-49]. In addition, such designs are explored for the normal wave incidence, whereas very little attention has been paid to the oblique incidence conditions [50-53]. In this work, we present forward and inverse deep learning models for modeling and designing metasurface absorbers, which address the issues and limitations mentioned earlier. To expand the design space, our approach

considers a large number of design DOFs and accounts for the two-dimensional (2D) geometrical pattern with complex freeform propagation channels, as well as properties like the thickness of the structure, and angle of incidence. Once fully trained with a sufficient amount of data, the proposed forward prediction network can generate accurate absorption coefficients of complex metasurface absorber structures for the given frequency. Practical applications of the metasurface absorber demand acoustic absorption effect at a particular frequency, which needs to realize design parameters that produce the customer-defined spectral response defined at the input. The goal of inverse design is to generate a working structure directly from the desired acoustic responses, eliminating the lengthy parameter scans or trial-and-error methods. Due to the extensive amount of design DOFs in non-intuitive metasurface patterns, the design scheme using CNN, such as backpropagation in trained simulator networks, is ineffective in the inverse design of metasurface. Furthermore, the trained CNN will always produce a fixed result for a given input. Meanwhile, multiple solutions may exist for the same target spectra fed to the simulator. To overcome these challenges, we implement a Conditional Generative Adversarial Network (CGAN). It is a conditional version of the generative adversarial network (GAN) whose generator and discriminator are conditioned during the training by using some additional information to direct the data generation process [54].

Using the proposed DNN methods, we demonstrate a metasurface absorber at 82Hz with nearly omnidirectional performance with a thickness of  $\lambda/64$ . The performance of the resulting metasurface absorber prototypes confirms that the implemented CNN and CGAN architectures achieves two important goals in the field of acoustic designs: (1) fast and accurate performance evaluation of complex structures for the oblique wave incidence at very low frequencies; and (2) finding non-intuitive designs based on predetermined acoustic response requirements. It is envisioned that the proposed approach also validates the feasibility of object-driven 3D acoustic device design which can be easily extended and generalized to many other acoustic device designs.

## 2. Structure Design of Acoustic Metasurface Absorber

The metasurface under evaluation is composed of a resonant cavity consist of freeform of propagation channel and cylindrical aperture covered by a plate of thickness  $t=1$  mm as shown in Figure 1(a). The embedded aperture is appended to the opening of the propagation channel. Such aperture and the propagation channel provide a feasible approach to tune the acoustic

impedance powerfully, thereby exhibiting superior capability and tunability for achieving desired absorption performances. The cell size is fixed at  $a=58$  mm and the thickness of the outer wall of the cavity is 2mm and thus, the lateral dimension of the square cavity is 56mm. The whole area of the square cavity is then decomposed into the square lattice sites of  $2\text{mm}\times 2\text{mm}$  to construct the propagation channel made of PLA (density,  $\rho = 2700 \text{ kg m}^{-3}$ ) with a thickness of 2mm.

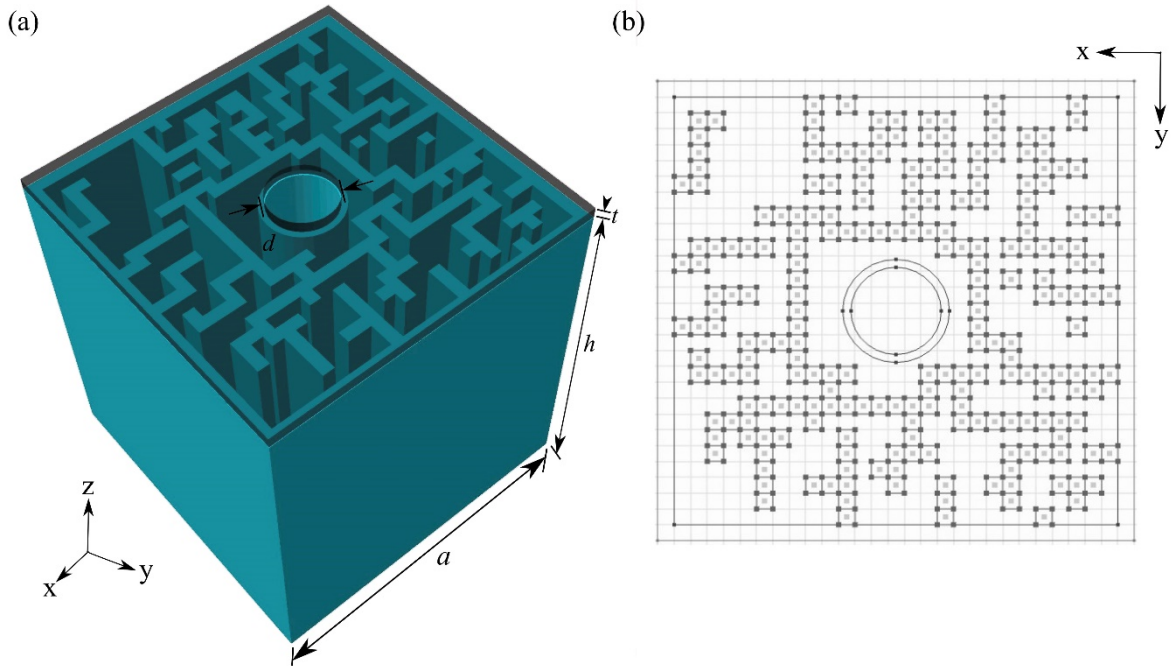


Figure 1-(a) Schematic of metasurface absorber (cross-area= $a\times a$  and whole thickness  $h+t$ ) for the oblique angle incidence. The full system includes a resonant cavity consisting of a freeform propagation channel (thickness  $h$ ) and cylindrical aperture (diameter  $d$ ). The cavity is covered by a plate with a centered hole (diameter  $d$ , thickness  $t$ ). (b) Top view of the system generated from the simulation software which is used as an input to the deep learning network.

The absorption responses of these structures were then calculated with the preset thermoviscous module of COMSOL Multiphysics v5.6. Hard boundary conditions are imposed on the air-structure interface due to a huge impedance mismatch. Over 9000 metasurface structures with different propagation channel shapes, diameter of hole, incidence angle, and thickness were generated within the following ranges (all dimensions are in mm and angles are in degree): thickness,  $h\in[65,75]$ , incidence angle  $\theta\in[0,60]$ , diameter of hole,  $d\in[10,12]$  since this range includes ample samples generating absorption resonance for the given frequency range. The height of the circular aperture is selected as  $(h-2)$  mm to take full advantage of the resonance to

achieve a lower frequency absorption. The spectra of interest are chosen as 80-100Hz for the purpose of demonstration. The whole spectrum is down sampled into 201 frequency points with a frequency step of 0.1Hz as the bandwidth of resonance is very narrow at a very low frequency. Here, the spectral response for the normal incidence is not influenced by the rotation of the structure. Hence, data augmentation is used by rotating 2D images by the random rotation and keeping their spectral response constant to generate more training data. It reduces the probability of the network overfitting the input data and also, increase the quantity and diversity in the training data. Before feeding to the network, the image data, associated properties, and corresponding acoustic response are cleaned and preprocessed (more details are included in the Supplementary Information, Section I).

### 3. Forward network architecture and results

We first construct a predicting neural network (PNN) based on a 2D CNN architecture for the forward design. The PNN aims to reveal the hidden relationship between the metasurface absorbers and their spectral response and thus accurately predict absorption responses for the given metasurface design. The proposed approach is not limited to particular shapes of the propagation channel and normal incidence only. We parameterized each metasurface structure's top view (2D pattern that includes the propagation channel and hole diameter), thickness, and angle of incidence. Later, they are concatenated as an input to the PNN. For feeding, the input data to the PNN, a batch generator is used that considerably lowers the RAM requirements. For any data, it randomly picks  $n$  rows ( $n$  is the batch size) and preprocesses them following which the batch input is fed to the network. As compared to total variables for our case, the training dataset size is small, and hence to help neural networks learn the patterns more easily, PCA is implemented using the 'scikit-learn' library. For our data, we use the first 20 components which explained 96.5% variance thus enabling us to reduce the dimensionality of the target absorption spectra from 201 to 20, i.e. 90% reduction.

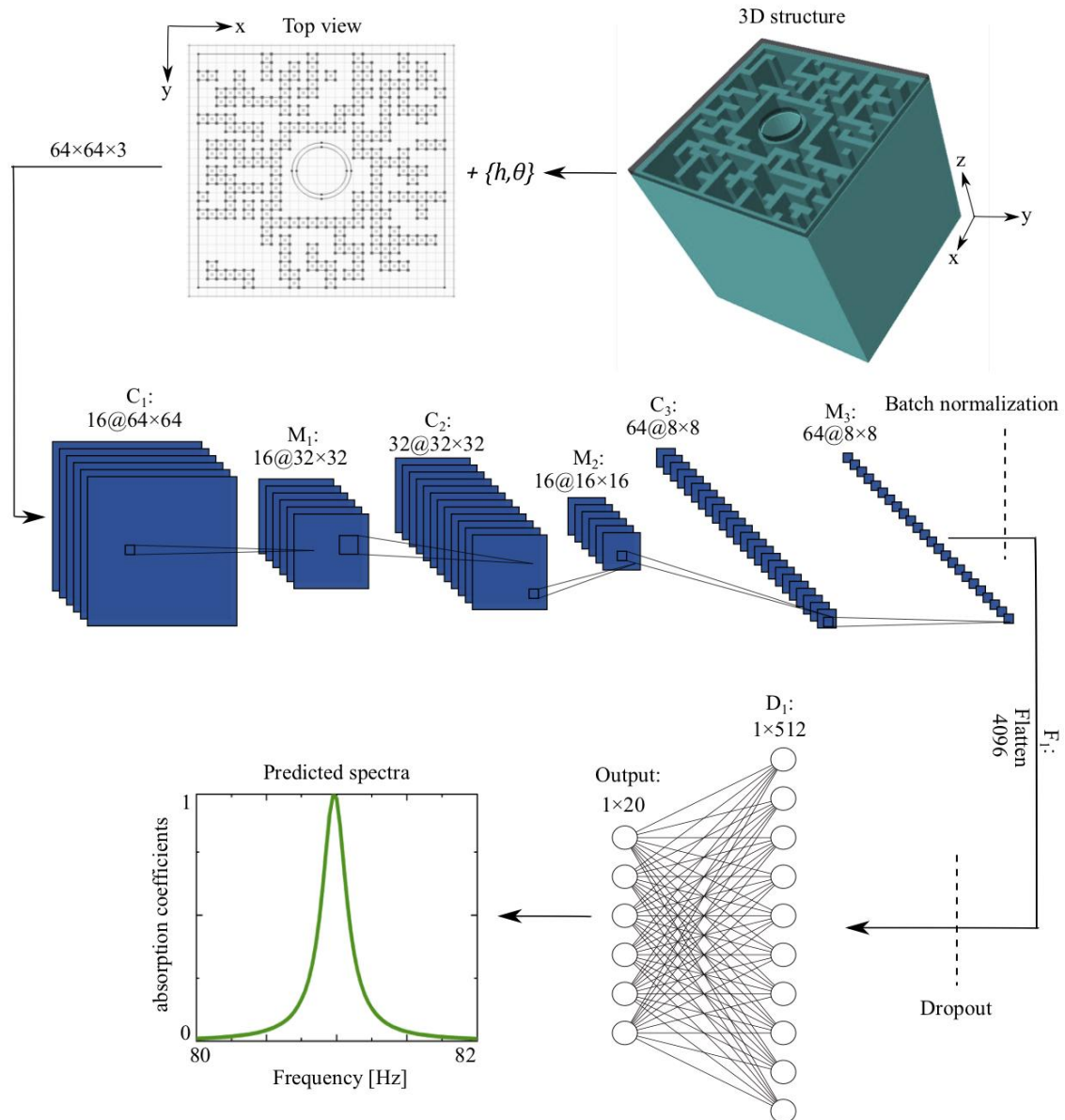


Figure 2- Illustration of the predicting network architecture (PNN) for the metasurface absorber design for oblique wave incidence. The input structure is divided into 1D properties and  $64 \times 64$  pixels 2D images. 1D properties are added to the 2D images as additional channels and both are processed through the same network. The output of the last max-pool layer,  $M_3$  is followed by a batch normalization layer before flattening. After being processed with two dense layers ( $D_1$  and output), the absorption spectra are ready for evaluation.

In prior work [55], good results were obtained by processing both 2D images and 1D properties (dimensions of the structure) using the separate networks and later concatenating and processing through the rest of the network. However, in our case, we find that the network shows overfitting when processing both properties separately. Therefore, we proposed a PNN that processes both in the same network by adding 1D properties (thickness and angle of

incidence) into 2D binary image composed of  $64 \times 64$  pixels as additional channels. The combined input is then fed to the PNN as illustrated in Figure 2. The input is passed sequentially through three combinations of convolution and max pooling layers ( $C_1-M_1-C_2-M_2-C_3-M_3$ ), each convolution layer having a kernel size of 3 and max pooling having the pool size of 2. The total number of filters used in the convolution layers are 16, 32, and 64 respectively. The output of layer  $M_3$  is passed through the batch normalization layer. Here, the aim of batch normalization is to accelerate the training process by reducing the internal covariate shift. Output of the batch normalization is passed through the flattening layer,  $F_1$  to flatten the output into single long feature vector. Before, feeding to the dense layers, a dropout is implemented to reduce the network overfitting issue. The output is then passed through a dense layer,  $D_1$  having 512 neurons followed by the output layer 20 neurons corresponding to components post PCA. At the output, we applied Rectified nonlinear activation function (ReLU) to introduce the nonlinearity in the network.

For the training process, the 9000 generated metasurface structures are split into training, validation, and test datasets, with 88% are used during the training process, 10% for the validation, and remaining 2% are used to evaluate the trained network. Figure 3(a) shows the learning curves (for the training and validation data), as a function of epochs. During the training phase, both the training and validation errors decreased and converged after 500 epochs. The network performance is quantified in term of mean squared error (MSE) which is given by,

$$MSE = \frac{1}{N} (\alpha_p - \alpha_s)^2 \quad (1)$$

where,  $\alpha_p$  and  $\alpha_s$  are the predicted and simulated absorption coefficients, respectively. When the training was finished, the average MSE was 0.00904 for the predicted absorption coefficients in the validation data. During the training process, the weights are continuously optimized to minimize the validation loss (the hyperparameters are included in the Supplementary Information, Section II). We then calculate the predicted spectra and compare the results to numerical simulations to extract the prediction error. To justify the usage of the batch normalization layer, and flatten layer in the PNN, we also carry out an ablation analysis (Supplementary Information, Section III). Results from this study indicates that including these layers improves the speed of convergence and accuracy.

To check the prediction accuracy of the trained model, we have evaluated it on the test dataset. Figure 3 (b)-(g) displays the example of some best fits in order to show the capability of the network. The results are shown for two different metasurface structures with different shapes of the propagation channel (inset in the plot (b) and (e)) with three different angles of incidence. For each case, the mean square error is listed in the inset. As indicated by the MSE, the absorption spectra predicted by the PNN (red dashed curves) agreed well with the FEM simulations (blue curves) for the variety of different propagation channels and different incidence angles. From the figures 3(b) to 3(d), it can be observed that the absorption peak is obtained at a very low frequency of 82Hz for the metasurface structure shown in the inset of the plot (b). The total thickness of the whole structure is as small as 1/64 of the working wavelength, which is much smaller than the previously reported acoustic absorbing metasurface designs for the oblique wave incidences [51,52]. The absorption for both structures is about 86% at  $\theta=60^\circ$  which shows overall good performance at large angles incidence.

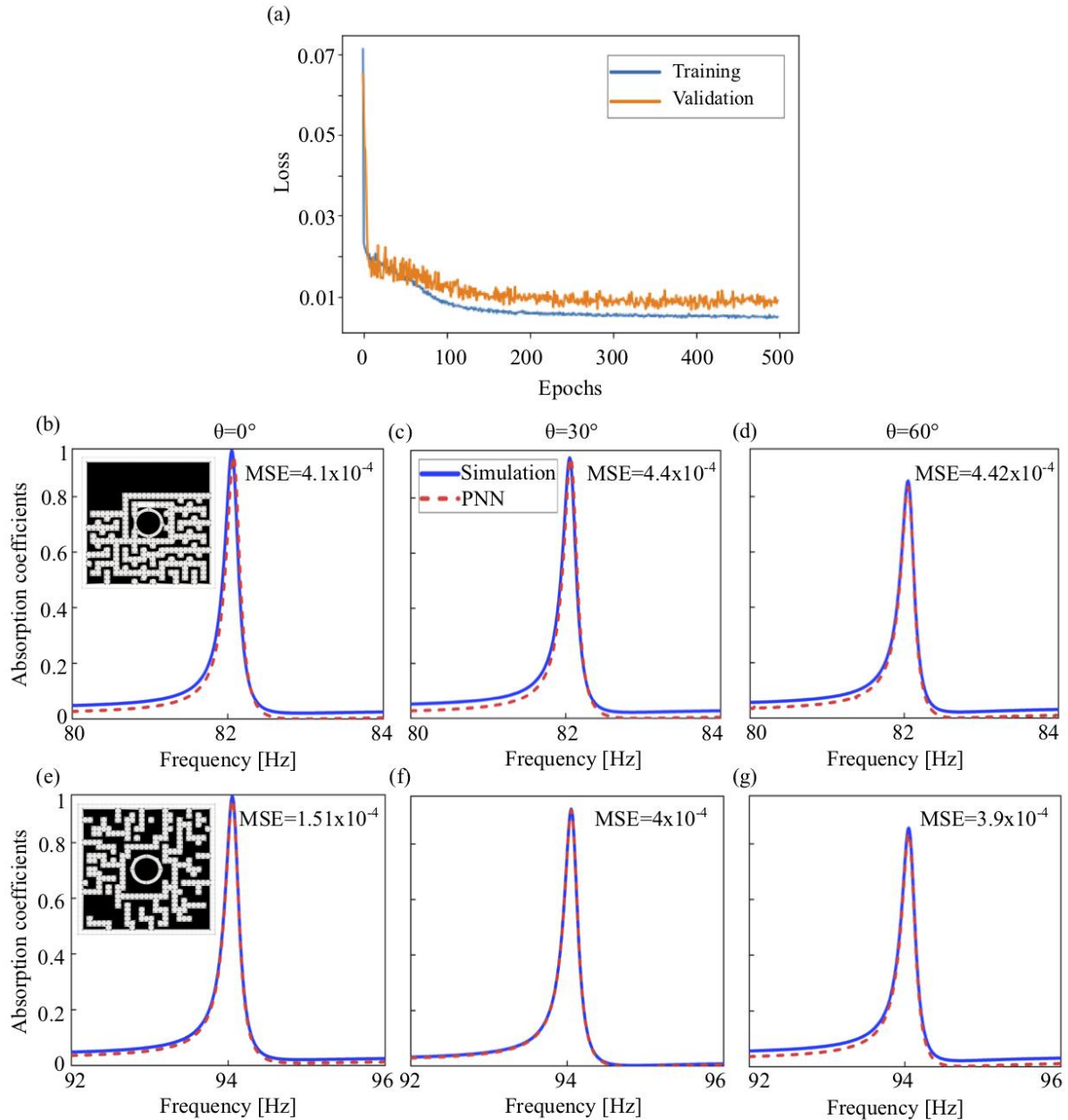


Figure 3 - (a) Learning curves as a function of epochs. (b)-(g) Comparison of PNN predicted absorption spectra (red dashed curves) with the simulated one (blue curves) for two different example metasurface structures with different shapes of the propagation channel (inset in the plot (b) and (e)). For each example, the comparison is shown for  $0^\circ$ ,  $30^\circ$ , and  $60^\circ$ . MSE of each case is included as insets.

#### 4. Inverse Network Architecture and Results

Practical applications of the metasurface absorber demand the perfect absorption at a particular frequency or frequency range which needs to generate specific design parameters to produce the desired absorption response using the inverse design. Once properly trained, the inverse

network should be able to excavate the best possible metasurface absorber design that yields absorption spectra with minimum deviation from the input absorption spectra. The development of such inverse design using the deep neural networks significantly reduces the computational time for design optimization.

To realize the inverse design, we have constructed the network architecture based on CGAN as shown in Figure 4(a). The aim of this network is to predict the metasurface structure for the prescribed absorption spectra and the thickness for the given incidence angle,  $\theta$ . The network is divided into two parts: a generator (G) and a discriminator (D). Both are convolutional neural networks with small differences in their detailed architecture. The generator is conditioned to produce images of new structures as a function of angle of incidence, thickness, and desired absorption spectra. The inputs to the generator are the incidence angle  $\theta$ , thickness  $h$ , desired absorption spectra  $A$ , and latent input space,  $z$  which comprises the number (latent size corresponding to the 2D pattern) of randomly chosen values between -1 to 1. Before feeding to the generator, the inputs are concatenated and passed through the dense layer for reshaping. The detailed architecture of the generator is shown in Figure 4(b). The reshaped input is passed through four transpose convolution layers  $CT_1$ ,  $CT_2$ ,  $CT_3$ ,  $CT_4$  with varying number of filters 128,32,16,1 and strides of 2,2,1,1 respectively. Such layers can be understood as the opposite of a pooling layer i.e. it increases the dimensions of the input and performs convolution after that to learn appropriate weights. Nonlinear activation function ReLU is applied after each the output of layers  $CT_1$ ,  $CT_2$ ,  $CT_3$ , and sigmoid activation function is applied at the output of the layer  $CT_4$ . A sigmoid activation is appropriate at the output of the layer as we want the discriminator's output to be 1 or 0.

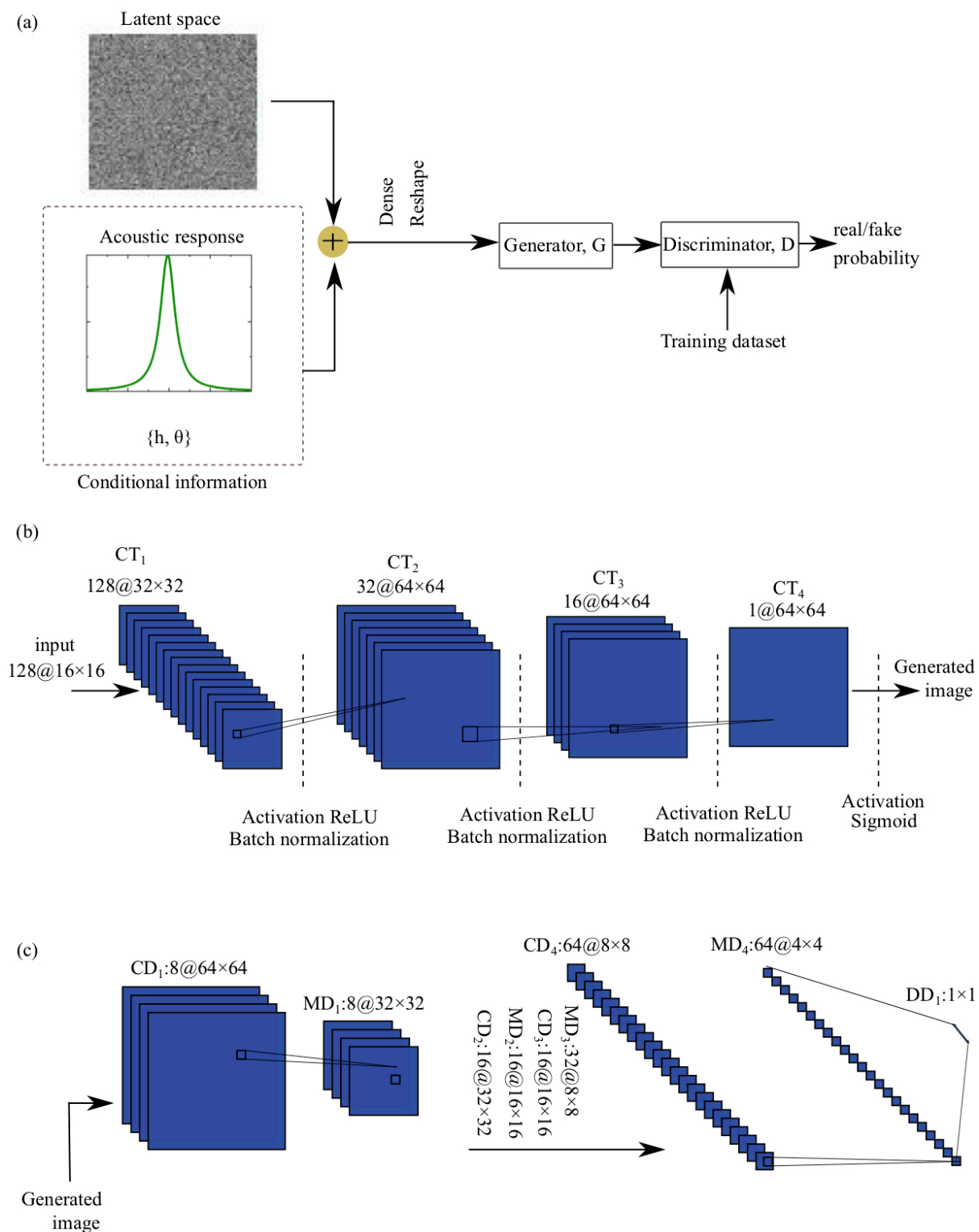


Figure 4- Illustration of the conditional generative adversarial network for the inverse metasurface absorber design for oblique wave incidence. (a) Schematic of the implemented network. (b) Detailed structure of the Generator (G). (c) Detailed structure of the Discriminator (D).

The discriminator, which is a classification network, learns to distinguish between image samples that come from the training dataset, and those from the generator. It accepts equally both the 2D images from the training dataset and the images generated from the generator. Our discriminator model is a convolutional neural network consisting of four convolution layers  $CD_1$ ,  $CD_2$ ,  $CD_3$ , and  $CD_4$  with the kernel size of 3 as shown in Figure 4(c). Each convolution layer uses 8, 16, 32, and 64 filters respectively with the stride of 1. Here, each convolution layer is followed by a max-pool layer ( $M_1$ ,  $M_2$ ,  $M_3$ ,  $M_4$ ) with the pooling size 2. We apply LeakyRELU activation functions in the layers of the discriminator network except for the final layer which is activated by a sigmoid function. The output of the last max-pool layer,  $M_4$  is flattened and fed to a fully connected layer having 1 neuron to generate the output i.e. 0 - image is fake, 1 - image is real. To prevent the networks from overfitting, a dropout layer is used in both the architectures.

The training process of the whole network for the one epoch can be explained as follows. To begin the training process, a batch is created which is a small group of the training dataset. It includes the latent space, the absorption spectra, and other properties from the training set. The generator creates the corresponding images based on the information in the batch. Here, as the inputs come from the randomized latent space,  $z$ , generation of the early images can be extreme noisy. Also, we have randomly initialized the parameters of the generator,  $G$ . In the next step, the same number of 2D images and corresponding absorption spectra are chosen from the training dataset. They are then mixed with the generator's predictions. Using this mixed subset, the discriminator learns to distinguish that the images are coming from the generator or training dataset. When the discriminator's output predicts either "fake" for a generator input (fake=0) or "real" for a training dataset input (real =1), it is considered true. The discriminator's parameters are updated and frozen after this step. Both the generator and discriminator are trained using the binary cross entropy loss function. Once the training of the CGAN is finished, the trained generator network is removed from it. Based on the desired input characteristics, appropriate metasurface absorber structure can be then tailored by the generator network.

As a demonstration of the proposed CGAN framework's overall competence, we use the absorption spectra,  $A$ , and other properties; thickness  $h$ , and angle of incidence  $\theta$ , randomly selected from the test data as input and ask the network to look for proper metasurface patterns based on these spectra. We denote this test set as  $s$ , the absorption spectra of each  $s$  as  $A$ . Once these spectra and other properties passed through the network, a 2D pattern is retrieved which

is denoted by  $s'$ . To verify the result, we simulate the generated set  $s'$  in COMSOL Multiphysics and denote the output spectra as  $A'$ . In Figure 5(a), the first row shows the sample from the test data,  $s$  and the second row show the corresponding samples  $s'$  generated by the CGAN. Each pair in two rows matches very well. Figure 5(b)-(e) show some best fits in order to demonstrate the capability of the network. Target designs of various metasurface absorbers and the corresponding suggested designs show good agreement.

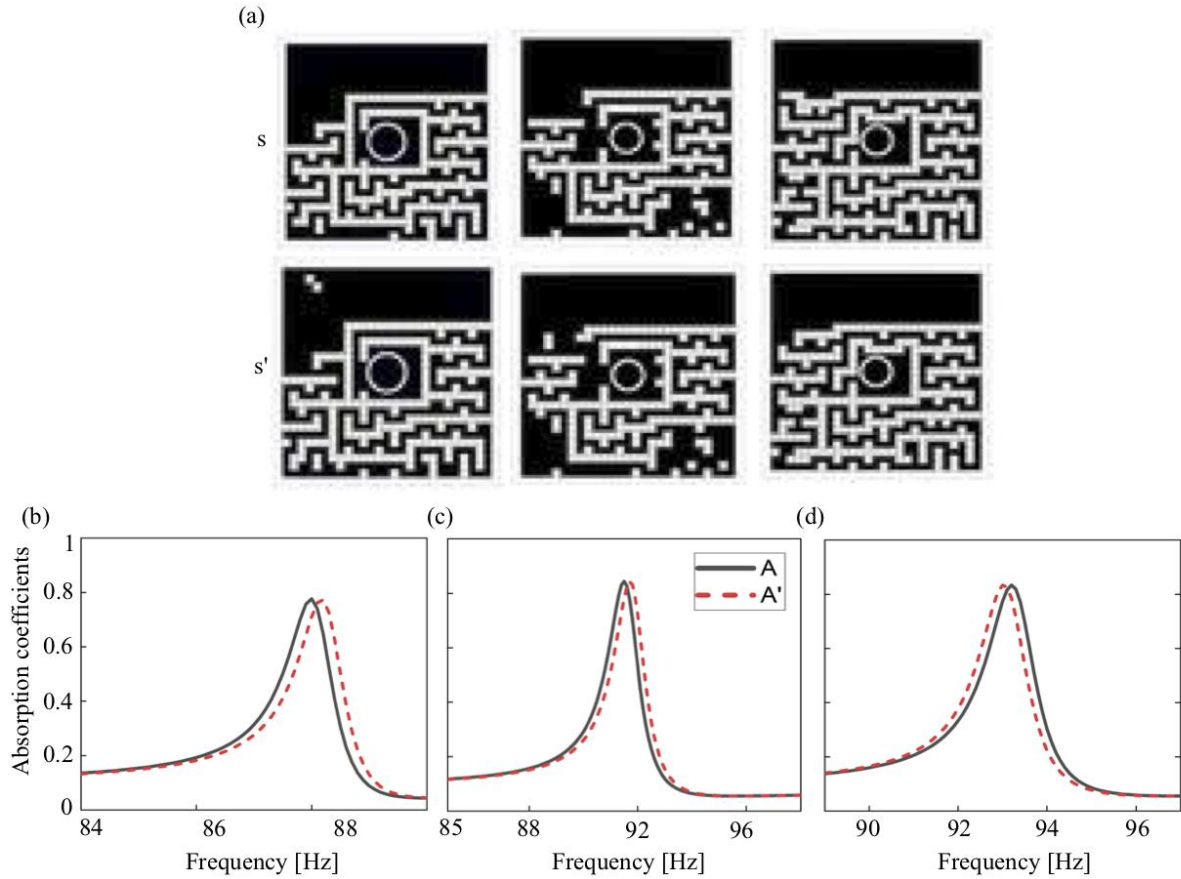


Figure 5: (a) 2D patterns  $s$  from the test dataset are shown in the top row and the corresponding generated patterns by CGAN are shown in the second row. (b) Comparison of the absorption spectra,  $A$  from the test set (black curve) and FEM simulated absorption spectra,  $A'$  of the retrieved pattern  $s'$  shown in the second row.

## Conclusion

In this research, a deep neural network based metasurface absorber designing approach for the oblique wave incidence is proposed and demonstrated. In particular, we have implemented CNN and CGAN for accurate forward and inverse design, respectively. Compared to the existing works, our approach can handle a large set of input parameters, including 2D patterns that contain freeform propagation channel and hole diameter, and other properties like thickness

and angle of incidence for the complex metasurface absorber structure. Using the presented CNN approach, we have conceived a metasurface absorber having nearly omnidirectional absorption at 82Hz with a thickness of  $\lambda/64$ . We have further implemented CGAN which can be adapted for designing metasurfaces with prescribed absorption spectra. The proposed deep learning approaches can be generically used for fast and accurate modeling and design process of the complex physical systems with minimum human intervention. We envision widespread and increasing use of deep learning methods in the field of physics, allowing scientists and engineers to focus more on truly creative ideas to solve the complex design problems that have yet to be explored by the machine, rather than on tedious trial and error processes.

### Data availability

The data that support the findings of this study are available from the corresponding author upon reasonable request.

### Acknowledgement

This work was supported by the Air Force Office of Scientific Research under Award No. FA9550-18-17021. The authors also acknowledge the support from la Region Grand Est.

### References

1. Assouar, B., Liang, B., Wu, Y., Li, Y., Cheng, J. C., & Jing, Y. (2018). Acoustic metasurfaces. *Nature Reviews Materials*, 3(12), 460-472.
2. Ma, G., & Sheng, P. (2016). Acoustic metamaterials: From local resonances to broad horizons. *Science advances*, 2(2), e1501595
3. Qi, S & Assouar, B. (2017). Acoustic energy harvesting based on multilateral metasurfaces. *Applied Physics Letters*, 111, 243506.
4. Xie, Y., Wang, W., Chen, H., Konneker, A., Popa, B. I., & Cummer, S. A. (2014). Wavefront modulation and subwavelength diffractive acoustics with an acoustic metasurface. *Nature communications*, 5(1), 1-5.
5. Assouar, B. Oudich, M & Zhou, X. (2016). Acoustic metamaterials for sound mitigation. *Comptes Rendus Physique*, 17, 524-532.

6. Li, Y., Jiang, X., Liang, B., Cheng, J. C., & Zhang, L. (2015). Metascreen-based acoustic passive phased array. *Physical Review Applied*, 4 (2), 024003.
7. Huang, S., Fang, X., Wang, X., Assouar, B., Cheng, Q., & Li, Y. (2018). Acoustic perfect absorbers via spiral metasurfaces with embedded apertures. *Applied Physics Letters*, 113(23), 233501.
8. Zhu, Y., Fan, X., Liang, B., Cheng, J., & Jing, Y. (2017). Ultrathin acoustic metasurface-based Schroeder diffuser. *Physical Review X*, 7(2), 021034.
9. Zhu, Y., & Assouar, B. (2019). Multifunctional acoustic metasurface based on an array of Helmholtz resonators. *Physical review B*, 99(17), 174109.
10. Li, Y., Liang, B., Gu, Z. M., Zou, X. Y., & Cheng, J. C. (2013). Reflected wavefront manipulation based on ultrathin planar acoustic metasurfaces. *Scientific reports*, 3(1), 1-6.
11. Xie, Y., Wang, W., Chen, H., Konneker, A., Popa, B. I., & Cummer, S. A. (2014). Wavefront modulation and subwavelength diffractive acoustics with an acoustic metasurface. *Nature Communications*, 5 (1), 1-5.
12. Li, Y., Liang, B., Tao, X., Zhu, X. F., Zou, X. Y., & Cheng, J. C. (2012). Acoustic focusing by coiling up space. *Applied Physics Letters*, 101(23), 233508.
13. Fan, S. W., Zhao, S. D., Chen, A. L., Wang, Y. F., Assouar, B., & Wang, Y. S. (2019). Tunable broadband reflective acoustic metasurface. *Physical Review Applied*, 11(4), 044038.
14. Cobo, P., Moraes, E., & Simón, F. (2015). Inverse estimation of the non-acoustical parameters of loose granular absorbers by Simulated Annealing. *Building and Environment*, 94, 859-866.
15. García-Chocano, V. M., Sanchis, L., Díaz-Rubio, A., Martínez-Pastor, J., Cervera, F., Llopis-Pontiveros, R., & Sánchez-Dehesa, J. (2011). Acoustic cloak for airborne sound by inverse design. *Applied physics letters*, 99(7), 074102.
16. Dong, J., Choi, K. K., & Kim, N. H. (2004). Design optimization for structural-acoustic problems using FEA-BEA with adjoint variable method. *J. Mech. Des.*, 126(3), 527-533.
17. Noguchi, Y., Yamada, T., Otomori, M., Izui, K., & Nishiwaki, S. J. A. P. L. (2015). An acoustic metasurface design for wave motion conversion of longitudinal waves to transverse waves using topology optimization. *Applied Physics Letters*, 107(22), 221909.

18. Noguchi, Y., & Yamada, T. (2021). Level set-based topology optimization for graded acoustic metasurfaces using two-scale homogenization. *Finite Elements in Analysis and Design*, 196, 103606.
19. Zhang, X., Xing, J., Liu, P., Luo, Y., & Kang, Z. (2021). Realization of full and directional band gap design by non-gradient topology optimization in acoustic metamaterials. *Extreme Mechanics Letters*, 42, 101126.
20. Noguchi, Y., & Yamada, T. (2021). Topology optimization of acoustic metasurfaces by using a two-scale homogenization method. *Applied Mathematical Modelling*.
21. Ahmed, W. W., Farhat, M., Zhang, X., & Wu, Y. (2021). Deterministic and probabilistic deep learning models for inverse design of broadband acoustic cloak. *Physical Review Research*, 3(1), 013142.
22. Weng, J., Ding, Y., Hu, C., Zhu, XF, Liang, B., Yang, J., & Cheng, J. (2020). Meta-neural-network for real-time and passive deep-learning-based object recognition. *Nature Communications* , 11 (1), 1-8.
23. Ciaburro, G., Iannace, G., Passaro, J., Bifulco, A., Marano, A. D., Guida, M., ... & Branda, F. (2020). Artificial neural network-based models for predicting the sound absorption coefficient of electrospun poly (vinyl pyrrolidone)/silica composite. *Applied Acoustics*, 169, 107472.
24. Zhao, T., Li, Y., Zuo, L., & Zhang, K. (2021). Machine-learning optimized method for regional control of sound fields. *Extreme Mechanics Letters*, 45, 101297.
25. Orazbayev, B., & Fleury, R. (2020). Far-field subwavelength acoustic imaging by deep learning. *Physical Review X*, 10(3), 031029.
26. Luo, Y. T., Li, P. Q., Li, D. T., Peng, Y. G., Geng, Z. G., Xie, S. H., ... & Zhu, X. F. (2020). Probability-density-based deep learning paradigm for the fuzzy design of functional metastructures. *Research*, 2020.
27. Donda, K., Zhu, Y., Merkel, A., Fan, S. W., Cao, L., Wan, S., & Assouar, B. (2021). Ultrathin Acoustic Absorbing Metasurface Based on Deep Learning Approach. *Smart Materials and Structures*.
28. Zhang, H., Wang, Y., Lu, K., Zhao, H., Yu, D., & Wen, J. (2021). SAP-Net: Deep learning to predict sound absorption performance of metaporous materials. *Materials & Design*, 212, 110156.
29. Ding, H., Fang, X., Jia, B., Wang, N., Cheng, Q., & Li, Y. (2021). Deep learning enables accurate sound redistribution via nonlocal metasurfaces. *Physical Review Applied*, 16(6), 064035.

30. Ivry, A., Cohen, I., & Berdugo, B. (2021). Nonlinear acoustic echo cancellation with deep learning. *arXiv preprint arXiv:2106.13754*.
31. Tran, T., Amirkulova, F., & Khatami, E. (2021). Acoustic cloak design via machine learning. *arXiv preprint arXiv:2111.01230*.
32. Sun, X., Jia, H., Yang, Y., Zhao, H., Bi, Y., Sun, Z., & Yang, J. (2021). Acoustic structure inverse design and optimization using deep learning. *arXiv preprint arXiv:2102.02063*.
33. Lai, P., Amirkulova, F., & Gerstoft, P. (2021). Conditional Wasserstein generative adversarial networks applied to acoustic metamaterial design. *The Journal of the Acoustical Society of America*, 150(6), 4362-4374.
34. Cheng, B., Wang, M., Gao, N., & Hou, H. (2022). Machine learning inversion design and application verification of a broadband acoustic filtering structure. *Applied Acoustics*, 187, 108522.
35. Wu, R. T., Jokar, M., Jahanshahi, M. R., & Semperlotti, F. (2022). A physics-constrained deep learning based approach for acoustic inverse scattering problems. *Mechanical Systems and Signal Processing*, 164, 108190.
36. Gurbuz, C., Kronowetter, F., Dietz, C., Eser, M., Schmid, J., & Marburg, S. (2021). Generative adversarial networks for the design of acoustic metamaterials. *The Journal of the Acoustical Society of America*, 149(2), 1162-1174.
37. Gao, N., Wang, M., Cheng, B., & Hou, H. (2021). Inverse design and experimental verification of an acoustic sink based on machine learning. *Applied Acoustics*, 180, 108153.
38. Mahesh, K., Kumar Ranjith, S., & Mini, R. S. (2021). Inverse design of a Helmholtz resonator based low-frequency acoustic absorber using deep neural network. *Journal of Applied Physics*, 129(17), 174901.
39. Kollmann, H. T., Abueidda, D. W., Koric, S., Guleryuz, E., & Sobh, N. A. (2020). Deep learning for topology optimization of 2D metamaterials. *Materials & Design*, 196, 109098.
40. Zhang, H., Wang, Y., Zhao, H., Lu, K., Yu, D., & Wen, J. (2021). Accelerated topological design of metaporous materials of broadband sound absorption performance by generative adversarial networks. *Materials & Design*, 207, 109855.
41. Shorten, C., & Khoshgoftaar, T. M. (2019). A survey on image data augmentation for deep learning. *Journal of Big Data*, 6(1), 1-48.

42. Perez, L., & Wang, J. (2017). The effectiveness of data augmentation in image classification using deep learning. *arXiv preprint arXiv:1712.04621*.
43. Bro, R., & Smilde, AK (2014). Main component analysis. *Analytical methods* , 6 (9), 2812-2831.
44. Li, Y., & Assouar, B. M. (2016). Acoustic metasurface-based perfect absorber with deep subwavelength thickness. *Applied Physics Letters*, 108(6), 063502.
45. Huang, S., Fang, X., Wang, X., Assouar, B., Cheng, Q., & Li, Y. (2019). Acoustic perfect absorbers via Helmholtz resonators with embedded apertures. *The Journal of the Acoustical Society of America*, 145(1), 254-262.
46. Donda, K., Zhu, Y., Fan, S. W., Cao, L., Li, Y., & Assouar, B. (2019). Extreme low-frequency ultrathin acoustic absorbing metasurface. *Applied Physics Letters*, 115(17), 173506.
47. Guo, J., Zhang, X., Fang, Y., & Jiang, Z. (2020). A compact low-frequency sound-absorbing metasurface constructed by resonator with embedded spiral neck. *Applied Physics Letters*, 117(22), 221902.
48. Kong, D., Huang, S., Li, D., Cai, C., Zhou, Z., Liu, B., ... & Liu, S. (2021). Low-frequency multi-order acoustic absorber based on spiral metasurface. *The Journal of the Acoustical Society of America*, 150(1), 12-18.
49. Shen, Y., Yang, Y., Guo, X., Shen, Y., & Zhang, D. (2019). Low-frequency anechoic metasurface based on coiled channel of gradient cross-section. *Applied Physics Letters*, 114(8), 083501.
50. Wu, X., Fu, C., Li, X., Meng, Y., Gao, Y., Tian, J., ... & Wen, W. (2016). Low-frequency tunable acoustic absorber based on split tube resonators. *Applied Physics Letters*, 109(4), 043501.
51. Ji, J., Li, D., Li, Y., & Jing, Y. (2020). Low-frequency broadband acoustic metasurface absorbing panels. *Frontiers in Mechanical Engineering*, 6, 94.
52. Liang, Q., Lv, P., He, J., Wu, Y., Ma, F., & Chen, T. (2021). A controllable low-frequency broadband sound absorbing metasurface. *Journal of Physics D: Applied Physics*.
53. Xu, Z. X., Meng, H. Y., Chen, A., Yang, J., Liang, B., & Cheng, J. C. (2021). Tunable low-frequency and broadband acoustic metamaterial absorber. *Journal of Applied Physics*, 129(9), 094502.
54. Mirza, M., & Osindero, S. (2014). Conditional generative adversarial nets. *arXiv preprint arXiv:1411.1784*.

55. An, S., Zheng, B., Shalaginov, M. Y., Tang, H., Li, H., Zhou, L., ... & Zhang, H. (2020). Deep learning modeling approach for metasurfaces with high degrees of freedom. *Optics Express*, 28(21), 31932-31942.